rhodium(II) spectra, these can be assigned as $\delta^*_{Rh_2} \rightarrow \sigma^*_{Rh_2}$ and MLCT transitions, respectively.

Summary. In this article we have outlined synthesis procedures for the replacement of bridging acetates of $Rh_2(OAc)_4$ by polydentate naphthyridine derivatives. The resulting complexes $Rh_2(OAc)_3L^+$, $Rh_2(OAc)_2L_2^{2+}$, and $Rh_2L_4^{4+}$ show intense absorption bands in the visible spectra, which have been tentatively assigned as metal to ligand charge-transfer bands. Several of these complexes display a very rich electrochemistry, undergoing both reversible oxidation and several reversible reductions as observed by cyclic voltammetry. The chemistry of these complexes, including potential catalyst applications, is under further investigation in these laboratories.

Contribution from Research Institute for Materials,
Faculty of Science, Toernooiveld, 6525 ED Nijmegen, The Netherlands

Intermediates in the Formation of Gold Clusters. Preparation and X-ray Analysis of [Au₇(PPh₃)₇]⁺ † and Synthesis and Characterization of [Au₈(PPh₃)₆I]PF₆

J. W. A. VAN DER VELDEN,* P. T. BEURSKENS, J. J. BOUR, W. P. BOSMAN, J. H. NOORDIK,
M. KOLENBRANDER, and J. A. K. M. BUSKES

The evaporation of metallic gold into a toluene solution containing PPh_3 (L) leads to the formation of a number of compounds from which the heptanuclear $[Au_7L_7]^+$ ($C_{126}H_{105}Au_7P_7^+$) can be isolated as the major constituent. An X-ray analysis has been performed on a single crystal, space group $P\bar{1}$, with cell dimensions $a = 34.94$ (1) Å, $b = 44.25$ (2) Å, $c = 15.45$ (1) Å, $\alpha = 99.98$ (3)°, $\beta = 102.66$ (3)°, $\gamma = 88.11$ (3)°, $V = 22\,953.5$ Å³, and $Z = 8$. The final R value is 0.099. The gold atoms in the $[Au_7L_7]^+$ cation form a slightly distorted pentagonal bipyramid, which is a novel feature for heptanuclear metal clusters. The axial Au–Au distance (average 2.584 ± 0.001 Å) is the shortest distance ever found in gold clusters. The axial–equatorial and equatorial–equatorial Au–Au distances have mean values of 2.82 ± 0.08 and 2.95 ± 0.06 Å, respectively. All P–Au vectors point approximately to the center of the cluster with normal P–Au distances (2.27 ± 0.09 Å). Physical data including ^{197}Au Mössbauer and (solid-state) ^{31}P{^{1}H} NMR are reported. $[Au_7L_7]^+$ can also be observed during the reaction of L with the novel compound $[Au_8L_6I]PF_6$. The latter cluster could be prepared from the reaction of $[Au_9L_8]^{3+}$ with Bu_4NI. The intermediacy of the title compounds in the formation and reactivity of gold cluster compounds will be discussed.

Introduction

The synthesis and the reactivity of gold phosphine clusters have been thoroughly studied during the last few years.[1] The fast formation of gold clusters containing 9 or 11 gold atoms by the reduction of Au(I) compounds can be observed under mild conditions, e.g., with ethanolic sodium borohydride as reducing agent at room temperature. Conversion reactions can occur for cationic gold phosphine clusters with Lewis bases, leading to other gold clusters within minutes. In particular, the reactions of $[Au_9L_8]^{3+}$ (L = PPh_3) have been studied intensively, showing that it can function as a starting material for the synthesis of gold clusters ranging in size from 4 to 11 gold atoms.[1] The presence of small intermediates, containing 2–4 Au atoms, has been suggested during both the formation and the conversion reactions of these compounds.

As the metal evaporation technique has proven to be a successful method for the synthesis of gold clusters in good yield,[2] we tried to isolate such a small intermediate from the reaction of gaseous gold atoms with L in toluene. This attempt was not successful, but led, however, to the discovery of a novel gold cluster compound, the heptanuclear $[Au_7L_7]^+$. ^{31}P{^{1}H}

NMR experiments show that it is also formed quantitatively in the reaction of excess L with $[Au_8L_6I]PF_6$, which is a novel product obtained from the reaction of $[Au_9L_8]^{3+}$ with Bu_4NI. The bruto formula and the structure of the Au_7 cluster were found by X-ray analysis. Physical data are provided from both novel compounds in this report.

Experimental Section

Measurements. Elemental analyses and molecular weight determinations were carried out in our microanalytical department and by Dr. A. Bernhardt, Elbach über Engelskirchen, West Germany. ^{31}P{^{1}H} NMR spectra were recorded on a Varian XL-100 FT (solution; ^{31}P, 40.5 MHz) or a home-built NMR instrument[3] (solid state; ^{31}P, 72.9 MHz), IR spectra on a Perkin-Elmer 283, ESR spectra on a Varian E12, and ^{197}Au Mössbauer spectra with the apparatus described earlier.[4] All solvents were of reagent grade and used without further purification.

---

† The identity of the anion is uncertain.

(1) Steggerda, J. J.; Bour, J. J.; van der Velden, J. W. A. *Recl. Trav. Chim. Pays-Bas* **1982**, *101*, 164.
(2) Vollenbroek, F. A.; Bouten, P. C. P.; Trooster, J. M.; van den Berg, J. P.; Bour, J. J. *Inorg. Chem.* **1978**, *17*, 1345.
(3) Veeman, W. S.; Menger, E. M.; Ritchey, W.; de Boer, E. *Macromolecules* **1979**, *12*, 924.
(4) Viegers, M. P. A.; Trooster, J. M. *Phys. Rev. B: Solid State* **1977**, *15*, 72.
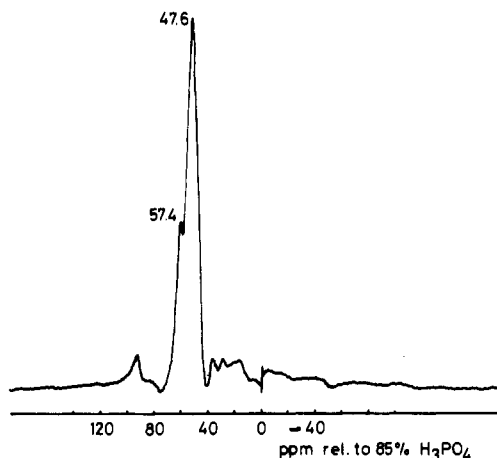
Figure 1. Solid-state $^{31}P\{^1H\}$ NMR spectrum of $[Au_7L_7]^+$.

Preparations. $[Au_9L_8](NO_3)_3$[5] (L = PPh$_3$) and $Au_4L_4(\mu\text{-}I)_2$[6] were prepared according to the literature.

Preparation of [Au7L7]+. With use of the rotary metal evaporation apparatus,[2] 800 mg of Au (ca. 4.0 mmol) was evaporated into 300 mL of toluene containing 1.60 g of L (ca. 6.1 mmol) at −100 °C, resulting in a dark red-brown slurry. After warming up to room temperature, the reaction mixture consisted of a brown solution and a brown solid. The latter could be isolated by filtration. The brown solid is washed with 20 mL of acetone from which by precipitation in 200 mL of petroleum ether (bp 40–60 °C) a compound is isolated, containing the $[Au_7L_7]^+$ cation and as yet an unidentified anion. A dark brown solid remained after filtration and washing with diethyl ether; yield 20–30% (based on Au). Crystals suitable for X-ray analysis could be obtained by slow diffusion of diethyl ether into an acetone solution. Since OH$^-$ is the most probable counterion (see below), it can be calculated that $[Au_7L_7](OH)$, has a molecular weight of 3231.838. Anal. Calcd for $C_{126}H_{106}Au_7OP_7$: C, 46.83; H, 3.31; Au, 42.66; P, 6.71; O, 0.50. Found: C, 43.94; H, 3.21; Au, 42.68; P, 6.70. Conductivity measurements in acetone indicate a 1:1 electrolyte (Λ_0 = 150 $\Omega^{-1}\cdot cm^2\cdot mol^{-1}$ from the extrapolation of Λ vs. $c^{1/2}$). $^{31}P\{^1H\}$ NMR (solution): sharp singlet (line width 3 Hz) at room temperature at 51.5 (CH_2Cl_2; with decomposition), 51.9 (THF), and 51.8 ppm (acetone) downfield relative to H_3PO_4 (85%)). $^{31}P\{^1H\}$ NMR (solid state): two overlapping peaks at 47.6 and 57.4 ppm downfield relative to 85% H_3PO_4 (Figure 1). The peak at 90 ppm is a spinning sideband. In the IR spectrum (KBr pellet), only bands originating from coordinated PPh$_3$ could be detected except for a weak broad band at 1600 cm^{-1}, which originates from the anion. The ESR spectrum shows no signal in the solid state or in solution (THF), as expected for a compound with an even number of electrons.

Preparation of [Au8L6I]PF6. A 0.50-g sample of $[Au_9L_8](NO_3)_3$ was dissolved in 20 mL of methanol, and the solution was cooled to −60 °C. A solution of excess Bu$_4$NI (0.45 g; mole ratio 1:10) in 10 mL of methanol was slowly added in about 5 min. The color of the reaction mixture remained dark red. A brick red solid was precipitated from this solution by adding the cold reaction mixture dropwise to a solution of 0.20 g of NH$_4$PF$_6$ in methanol (50 mL). The process of precipitation can be accelerated by the addition of water. The precipitate was isolated by filtration. To remove any traces of Bu$_4$NI, it was washed with a mixture of methanol/water (70/30): yield 0.40 g (85% based on Au); $[Au_8L_6I]PF_6$, M_r = 3421.383. Anal. Calcd for $C_{108}H_{90}Au_8F_6IP_7$: C, 37.91; H, 2.65; Au, 46.06; F, 3.33; I, 3.71; P, 6.34. Found: C, 38.18; H, 2.57; Au, 46.23; F, 3.38; I, 3.66; P, 5.26. Electrical conductivity measurements in acetone and Me$_2$SO indicate a 1:1 electrolyte (Λ_0 (in acetone) = 101 $\Omega^{-1}\cdot cm^2\cdot mol^{-1}$ and (in Me$_2$SO) 24 $\Omega^{-1}\cdot cm^2\cdot mol^{-1}$ from the extrapolation of Λ vs. $c^{1/2}$). By the osmometric pressure procedure the apparent molecular weight was found to be 1710 in acetone. Assuming a 1:1 electrolyte, we obtain for the real molecular weight 3420 (calcd 3421.383). In the IR spectrum (CsI pellet), only bands originating from coordinated PPh$_3$

(5) Cariati, F.; Naldini, L. *J. Chem. Soc., Dalton Trans.* **1972**, 2286. van der Velden, J. W. A.; Bour, J. J.; Noordik, J. H.; Bosman, W. P., to be submitted for publication in *Inorg. Chem.*

(6) Demartin, F.; Manassero, M.; Naldini, L.; Ruggeri, R.; Sansoni, M. *J. Chem. Soc., Chem. Commun.* **1981**, 222.

Table I. ^{197}Au Mössbauer Parameters of $[Au_7L_7]^+$ and $[Au_8L_6I]PF_6$

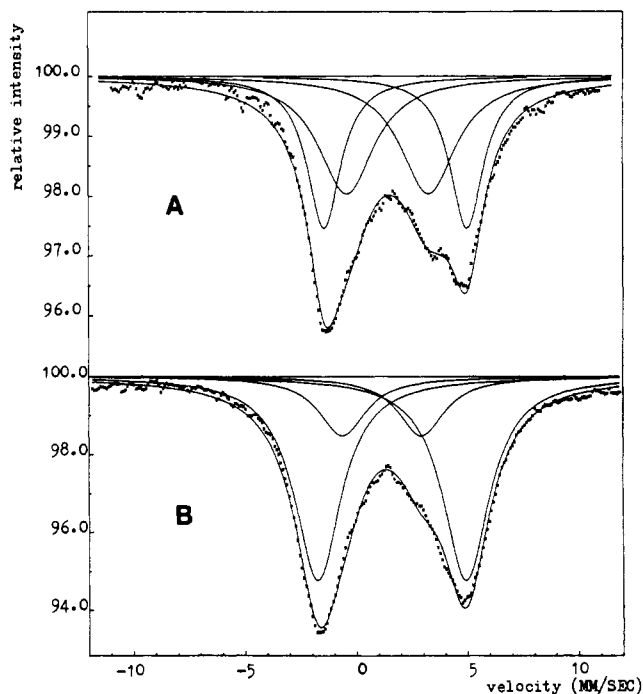| compd	Au site	QS, mm/s	IS,[a] mm/s	line width, mm/s	rel intens
$[Au_7L_7]^+$	axial	4.12	1.48	3.70	1
	equatorial	6.95	1.95	2.06	1.18
$[Au_8L_6I]PF_6$	Au-P	6.65	1.58	2.72	3.56
	Au-I	3.48	1.03	2.72	1

[a] IS relative to ^{197}Pt source.

Figure 2. ^{197}Au Mössbauer spectra of $[Au_7L_7]^+$ (A) and $[Au_8L_6I]PF_6$ (B).

and PF$_6^-$ could be detected. The ESR spectrum shows no signal, as expected for a cluster of this type with an even number of electrons. The ^{197}Au Mössbauer spectrum could be fitted with two quadrupole pairs (Figure 2 and Table I). According to the Mössbauer parameters and the relative intensities of these two pairs, the one with the largest intensity was assigned to the gold atoms to which the phosphines are bonded and the other to the gold atom coordinated to the iodine. $^{31}P\{^1H\}$ NMR (CH_2Cl_2): a sharp singlet (line width 3 Hz) at room temperature at 56.4 ppm downfield relative to H_3PO_4 (85%). $^{31}P\{^1H\}$ NMR (solid state): only a broad peak (line width 1460 Hz) at 56.0 ppm downfield relative to 85% H_3PO_4.

Crystal Structure Determination of $[Au_7(PPh_3)_7]^+$

Collection of the Reflection Intensities. Crystallographic data of a brown-red crystal of 0.4 × 0.1 × 0.05 mm were collected (at room temperature) on a single-crystal Nonius CAD-4 diffractometer using Mo Kα radiation (λ = 0.709 30 Å) and monochromated with a graphite-crystal monochromator. The unit cell dimensions were calculated from the setting angles of 25 reflections having $16° < 2\theta < 22°$. The lattice constants are a = 34.94 (1) Å, b = 44.25 (2) Å, c = 15.45 (1) Å, α = 99.98 (3)°, β = 102.66 (3)°, γ = 88.11 (3)°, and V = 22953.5 Å^3 in space group $P\bar{1}$, with p_{calcd} = 1.87 g·cm^{-3}, Z = 8, and linear absorption coefficient μ(Mo Kα) = 93.4 cm^{-1}. The data were collected by using the ω–2θ scan with a variable scan speed with a maximum time of 40 s per reflection. A total of 8659 reflections (slightly more than one-half sphere, with $2\theta < 22°$) were recorded. Three standard reflections were measured after every 1800 s of X-ray exposure time. Their intensities remained constant within 1%. After equivalent reflections (R_{av} = $\sum(||I| - |\bar{I}||)/\sum|I|$ = 0.016) were averaged, 7408 reflections remained of which 4787 had $I > 3\sigma(I)$ ($\sigma(I)$ based on counting statistics). The intensities were corrected for Lorentz and polarization effects and reduced to $|F_0|$ values. Absorption and extinction corrections were not applied.

Table II. Positional and Thermal Parameters ($\times 100$, Å^2) for the Au_7P_7 Clusters (esd's within Parentheses)

	x (± 0.0003)	y (± 0.0002)	z (± 0.0007)	U_{eq}		x (± 0.002)	y (± 0.001)	z (± 0.005)	U_{eq}
Au(11)	0.1038	0.1785	0.1528	2.1 (8)	P(11)	0.159	0.177	0.271	2 (5)
Au(12)	0.0430	0.1825	0.0257	1.4 (5)	P(12)	−0.010	0.188	−0.085	5 (0)
Au(13)	0.0311	0.1765	0.2007	3.0 (9)	P(13)	0.002	0.167	0.313	7 (6)
Au(14)	0.0557	0.1256	0.0822	2.7 (5)	P(14)	0.037	0.076	0.060	6 (6)
Au(15)	0.1044	0.1488	−0.0267	4.0 (9)	P(15)	0.139	0.125	−0.117	6 (5)
Au(16)	0.1105	0.2161	0.0306	2.6 (8)	P(16)	0.153	0.249	−0.006	4 (7)
Au(17)	0.0573	0.2336	0.1586	5.7 (9)	P(17)	0.037	0.284	0.202	12 (8)
Au(21)	0.4571	0.3181	0.8001	3.3 (5)	P(21)	0.513	0.310	0.736	4 (5)
Au(22)	0.3961	0.3215	0.8700	3.5 (9)	P(22)	0.345	0.322	0.932	1 (5)
Au(23)	0.3890	0.2838	0.7027	3.1 (8)	P(23)	0.346	0.254	0.593	4 (6)
Au(24)	0.3961	0.3515	0.7213	3.2 (8)	P(24)	0.361	0.377	0.616	3 (5)
Au(25)	0.4442	0.3745	0.9008	2.7 (9)	P(25)	0.468	0.422	0.949	4 (6)
Au(26)	0.4684	0.3238	0.9936	2.6 (8)	P(26)	0.495	0.335	0.151	8 (6)
Au(27)	0.4421	0.2662	0.8668	6.0 (9)	P(27)	0.465	0.217	0.879	8 (6)
Au(31)	0.8449	0.4433	0.7847	3.4 (9)	P(31)	0.878	0.445	0.907	4 (6)
Au(32)	0.8004	0.4404	0.6259	4.9 (9)	P(32)	0.758	0.435	0.482	3 (5)
Au(33)	0.7680	0.4555	0.7858	5.0 (9)	P(33)	0.720	0.470	0.865	4 (5)
Au(34)	0.7943	0.3936	0.7268	4.9 (9)	P(34)	0.762	0.350	0.703	5 (6)
Au(35)	0.8681	0.3953	0.6632	7.1 (9)	P(35)	0.904	0.356	0.608	4 (5)
Au(36)	0.8824	0.4602	0.6635	3.6 (5)	P(36)	0.927	0.477	0.607	6 (6)
Au(37)	0.8223	0.4986	0.7314	4.1 (9)	P(37)	0.815	0.552	0.742	6 (5)
Au(41)	0.3004	0.9400	0.6148	5.3 (9)	P(41)	0.257	0.938	0.701	7 (6)
Au(42)	0.3446	0.9428	0.5025	4.0 (9)	P(42)	0.382	0.945	0.402	6 (6)
Au(43)	0.2684	0.9553	0.4385	4.4 (9)	P(43)	0.218	0.970	0.323	2 (4)
Au(44)	0.2950	0.8942	0.4628	5.4 (9)	P(44)	0.264	0.851	0.404	12 (9)
Au(45)	0.3670	0.8955	0.6002	6.5 (9)	P(45)	0.403	0.854	0.651	10 (7)
Au(46)	0.3830	0.9600	0.6789	4.2 (9)	P(46)	0.431	0.976	0.795	6 (6)
Au(47)	0.3222	0.9990	0.5903	4.2 (8)	P(47)	0.312	0.051	0.625	4 (5)

^{a} $U_{eq} = \frac{1}{3}\Sigma_i\Sigma_j a_i a_j U_{ij}$.

Solution of the Structure. The structure, consisting of at least 560 symmetry-independent non-hydrogen atoms, was solved by successive applications of Patterson, DIRDIF,[7-10,26] and Fourier techniques. Final parameters were obtained by alternative application of full-matrix least-squares refinement to individual blocks of $P(C_6)_3$ and Au_7P_7, with restrained phenyl rings, allowing anisotropic vibration for the gold and phosphorus atoms. The weights used are $w = [\sigma_c^2(F_0) + 0.0015F_0^2]^{-1}$. This gave $R = 0.099$ and $R_w = 0.14$ for 617 variable parameters and 4787 "observed" reflections. Scattering factors were taken from ref 10 with use of the anomalous dispersion term f' for gold.

A difference Fourier synthesis showed some residual electron density around the gold atoms and about 17 peaks at positions in the tetrahedral and octahedral cavities between the clusters. Contact distances between the peaks are in the range 2.0–3.0 Å. The 15 strongest peaks were denoted oxygen and subjected to least-squares refinement; the population parameters converged to values in the range 0.5–1.2. Inspection of the difference map showed that the peaks belonged to regions of electron density that can be associated with disordered collections of $(H_2O)_nOH^-$, acetone, and/or diethyl ether (see preparation); a more accurate determination of those electron densities was not possible. (See also Figure 3.)

Positional and thermal parameters of the four Au_7P_7 clusters are given in Table II; selected bond distances and angles are provided in Table III. Structure factor tables and the positional parameters of the phenyl carbon atoms and of the residual peaks between the clusters (see above) are available as supplementary material.

Results and Discussion

[Au_8L_6I]⁺, an Intermediate in the Formation of $Au_4L_4(\mu$-I)$_2$. Several years ago it was shown that the reactions of [Au_9L_8]³⁺ with (pseudo)halides X^- ($X^- = Cl^-$, I^-, CN^-, or SCN^-) in CH_2Cl_2 can lead to the fast formation of Au_{11} clusters.[11]

(7) van den Hark, T. E. M.; Prick, P. A. J.; Beurskens, P. T. *Acta Crystallogr., Sect. A* **1976**, *A32*, 816.

(8) Prick, P. A. J.; Beurskens, P. T.; Gould, R. O. *Acta Crystallogr., Sect. A* **1978**, *A34*, S42.

(9) Doesburg, H. M.; Beurskens, P. T. *Acta Crystallogr., Sect. A* **1981**, *A37*, C327.

(10) Cromer, D. T.; Waber, J. T. "International Tables for X-ray Crystallography"; Kynoch Press: Birmingham, England, 1974; Vol. IV, Table 2.2b, 2.3.1.

Table III. Selected Bond Distances (Å) and Angles (deg) for One of the [Au_7L_7]⁺ Clusters (Esd's within Parentheses)

Au–Au (± 0.02)			
21–22	2.58	22–25	2.84
21–23	2.85	22–26	2.81
21–24	2.74	22–27	2.88
21–25	2.78	23–24	2.97
21–26	2.90	23–27	3.00
21–27	2.78	24–25	2.94
22–23	2.79	25–26	2.87
22–24	2.85	26–27	2.97

Au–P (± 0.06)			
21–22	2.36	25–25	2.22
22–22	2.20	26–26	2.38
23–23	2.26	27–27	2.33
24–24	2.26		

Au–Au–Au (± 0.4)			
22–21–23	61.6	24–23–27	106.3
22–21–24	64.6	23–24–25	107.9
22–21–25	63.9	24–25–26	109.4
22–21–26	61.4	25–26–27	108.1
22–21–27	64.9	26–27–23	107.4

Au–Au–P (± 2)			
22–21–21	175	21–25–25	143
21–22–22	177	21–26–26	163
21–23–23	163	21–27–27	142
21–24–24	157		

More recently, the study of the reactivity of [Au_9L_8]³⁺ toward Lewis bases showed that the majority of the known clusters and a series of novel cluster compounds could be prepared conveniently from [Au_9L_8]³⁺ by conversion reactions.[1]

The remarkable reactivity of [Au_9L_8]³⁺ can be ascribed to the dissociation of an [AuL]⁺ ion in solution, leaving the coordinatively unsaturated [Au_8L_7]²⁺. The latter cluster could be isolated, and its intermediacy has been demonstrated in the [Au_9L_8]³⁺ ↔ [Au_8L_8]²⁺ interconversion reaction. Association of 1 equiv of [AuL]⁺ or L leads instantaneously to the for-

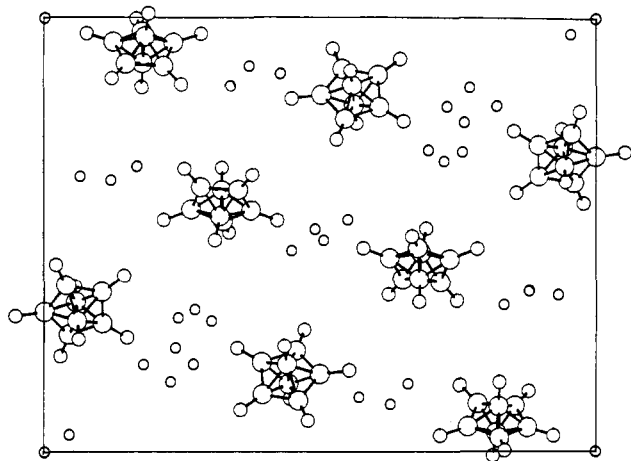(11) Vollenbroek, F. A.; Bour, J. J.; van der Velden, J. W. A. *Recl. Trav. Chim. Pays-Bas* **1980**, *99*, 137.

Figure 3. Projection of the unit cell along the c axis, showing the eight Au₇P₇ clusters and the "oxygen" atoms.

mation of [Au₉L₈]³⁺ and [Au₈L₈]²⁺, respectively.[5]

As reported by Demartin et al.,[6] [Au₉L₈]³⁺ reacts with KI in acetone toward the tetrahedral Au₄L₄(μ-I)₂. Duplicating this experiment, we also found a red product that decomposed after some time, leaving only Au₄L₄(μ-I)₂, some gold metal, and AuLI. As we believed this red product to be an intermediate in this reaction, we carried out the reaction at −60 °C by dissolving [Au₉L₈]³⁺ in methanol and adding a 10-fold excess of Bu₄NI in methanol to this solution. A pure red product, identical with the one mentioned above in the Au₄L₄(μ-I₂) synthesis, could be isolated; the analytical data are in agreement with the formula [Au₈L₆I]PF₆. Furthermore, when [Au₈L₆I]PF₆ is dissolved in acetone in the presence of KI, Au₄L₄(μ-I)₂ is formed together with some gold metal and AuLI, showing the intermediacy of [Au₈L₆I]PF₆ in the conversion of [Au₉L₈]³⁺ with KI to Au₄L₄(μ-I)₂.

The formation of this novel octanuclear cluster can be thought to proceed by the substitution of a phosphine by an iodine in the [Au₈L₇]²⁺ cluster, which probably acts also as an intermediate in this reaction. The [Au₈L₆I]⁺ cation might be isostructural with [Au₈L₇]²⁺. This can be concluded from the ¹⁹⁷Au Mössbauer spectrum (Figure 2B), which could be fitted reasonably well with two quadrupole pairs attributable to a gold–phosphine site and a gold–iodine site, respectively, without a separately observable central gold atom. This latter phenomenon also occurs for [,au₈L₇]²⁺ and [Au₉L₈]³⁺, which have very similar structures. In contrast, [Au₈L₈]²⁺ shows a definitely observable singlet for the central gold atom. This difference can be accounted for in terms of a more symmetric population in the Au 6p levels, as will be reported more fully in a forthcoming paper.[12]

Description of the Crystal and Molecular Structure of [Au₇L₇]⁺. The unit cell contains eight heptanuclear [Au₇L₇]⁺ cations, of which four are symmetry related under space group $P\bar{1}$ (Figure 3). All cluster cations are very similar, with no unusual inter- or intramolecular short contacts.

The Au skeleton is a pentagonal bipyramid, which is a novel feature for heptanuclear clusters (Figure 4). Averaged Au–Au distances are (i) axial–axial 2.584 ± 0.008 Å, (ii) axial–equatorial 2.82 ± 0.08 Å, and (iii) equatorial–equatorial 2.95 ± 0.06 Å. The axial–axial distance is the shortest distance ever found in gold clusters and indicative of a strong interaction. In the group of centered gold clusters containing 8, 9, 11, or 13 gold atoms,[1] the radial bonds have values in the range 2.62–2.72 Å, while the peripheral bonds are in the range 2.8–3.1 Å, which comprises the bond lengths we found for the
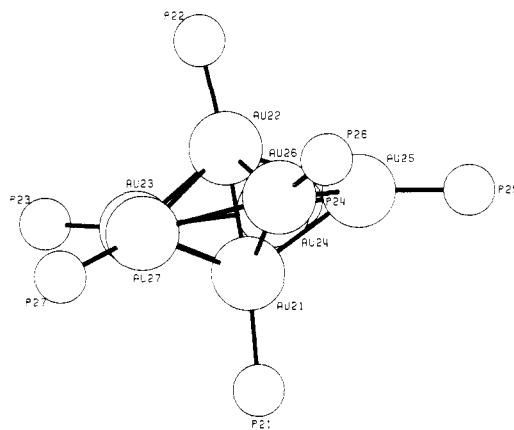

Figure 4. Au–P skeleton for one of the [Au₇L₇]⁺ cations with numbering scheme.
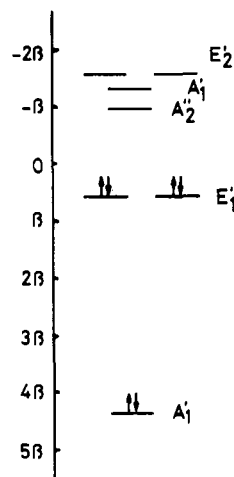

Figure 5. Hückel MO scheme for the Au₇ skeleton considering only Au 6s–6s overlaps for neighboring atoms.

above-mentioned groups ii and iii. All P–Au vectors in [Au₇L₇]⁺ point approximately to the center of the cluster with normal P–Au distances (2.27 ± 0.09 Å). The total Au₇P₇ skeleton deviates slightly from the pentagonal bipyramid.

Remarks on the Ionic Charge and the Cluster Geometry of [Au₇L₇]⁺. As stated above, the pentagonal bipyramid is a novel feature for heptanuclear metal clusters. In contrast with clusters containing six or less metal atoms, heptanuclear clusters are not abundant, and the few examples that are known all have capped-octahedral geometries, e.g., OS₇(CO)₂₁[13] and [Rh₇(CO)₁₆]³⁻.[14] The latter geometry agrees with the electron-counting scheme for clusters,[15] predicting capped-closo geometries for n-vertex polyhedra with $2n$ skeletal electrons. These electron-counting schemes cannot be applied for gold clusters. (EH)MO calculations can be used to predict quite successfully the number of valence electrons in the metal skeleton and thereby the ionic charge of a gold cluster.[11,16]

A simple Hückel MO calculation on the pentagonal-bipyramidal Au₇ skeleton, involving only Au 6s–6s overlaps of neighboring atoms, shows that six electrons can be accommodated in three bonding MO's, confirming the 1+ charge of the Au₇L₇ cluster (Figure 5).

(12) van der Velden, J. W. A.; Stadnik, Z. M., submitted for publication in *J. Am. Chem. Soc.*

(13) Eady, C. R.; Johnson, B. F. G.; Lewis, J. *J. Organomet. Chem.* **1972**, *37*, C39. Eady, C. R.; Johnson, B. F. G.; Lewis, J.; Mason, R.; Hitchcock, P. B.; Thomas, K. M. *J. Chem. Soc., Chem. Commun.* **1977**, 385.

(14) Albano, V. G.; Bellon, P. L.; Ciani, G. F. *J. Chem. Soc. D* **1969**, 1024.

(15) Wade, K. *Adv. Inorg. Chem. Radiochem.* **1976**, *18*, 1. Rudolph, R. W. *Acc. Chem. Res.* **1976**, *9*, 446. Mingos, D. M. P. *Nature (London)* **1972**, *236*, 99. Mingos, D. M. P.; Forsyth, M. J. *J. Chem. Soc., Dalton Trans.* **1977**, 610.

(16) Mingos, D. M. P. *J. Chem. Soc., Dalton Trans.* **1976**, 1163.

Several authors have indicated that all centered gold clusters can be considered to be derived from the isosahedron.[1] Although $[Au_7L_7]^+$ is not centered, it can also be described as an icosahedron from which one pentagonal pyramid has been removed. The displayed 5-fold symmetry does not occur frequently in molecular metal clusters. Usually, the metal frameworks are close-packed arrangements of atoms, e.g., $[Rh_{13}(CO)_{24}H_3]^{2-}$[17] and $[Pt_3(CO)_6]_n{}^{2-}$ (n = 2–6, 10).[18] An example of a cluster with pentagonal symmetry is $[Pt_{19}(CO)_{12}]^{4-}$.[19]
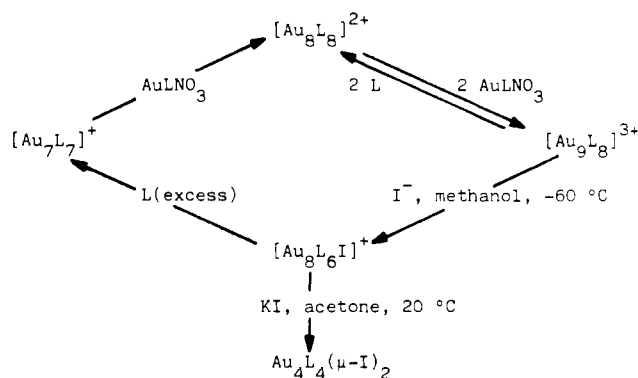
Icosahedral growing routes have been shown to exist from electron microscope studies[20] on small gold particles deposited on mica. Also, it was predicted from molecular dynamics calculations[21] on microclusters that icosahedrally derived structures are favored; for a heptanuclear cluster, the pentagonal bipyramid has been predicted.

[197]Au Mössbauer and ^{31}P{^{1}H} NMR Spectra of the $[Au_7L_7]^+$ Cluster. The [197]Au Mössbauer and the solid-state ^{31}P{^{1}H} NMR spectra of $[Au_7L_7]^+$ agree fully with the presence of two sets of different Au and P atoms (Figure 1 and 2). For centered gold clusters, the peripheral gold atoms give rise to a Mössbauer doublet for which the isomer shift (IS) and quadrupole splitting (QS) depend on the type of ligand to which it is bonded. For these clusters, geometrical site differences have no detectable influence.[22] Thus, the peripheral gold atoms in $Au_{11}L_7X_3$ and $[Au_{11}L_8X_2]^+$ (X = (pseudo)-halide) give rise to two quadrupole pairs in their Mössbauer spectrum, while those in $[Au_{11}(PPh_2[CH_2]_3PPh_2)_5]^{3+}$, $[Au_9L_8]^{3+}$, $[Au_8L_8]^{2+}$, and $[Au_8L_7]^{2+}$ give rise to only one quadrupole pair.[22-24] The presence of two quadrupole pairs for $[Au_7L_7]^+$ thus indicates a quite unusual difference between the axial and the equatorial gold atoms. The Mössbauer parameters suggest a more spherical surrounding for the axial gold atoms when compared to the equatorial gold atoms. In comparison with the Mössbauer parameters for centered gold clusters, the axial gold atoms seem to be less spherically surrounded as, e.g., the central gold atom in $[Au_8L_8]^{2+}$, while the equatorial gold atoms are similar to the peripheral gold phosphine sites in the centered gold clusters. These observations are in agreement with results from EHMO calculations as will be reported in a forthcoming paper.[12]

Reactivity and Formation of Gold Cluster Compounds. The product obtained in the preparation of gold clusters depends on the coordinating ability of the anions that are present in the reaction mixture and on the steric demands of the phosphine.[1] With PAr_3 (Ar = phenyl or monosubstituted aryl) and noncoordinating anions, $[Au_9L_8](NO_3)_3$ is formed. When strongly coordinating anions X such as I^-, Cl^-, CN^-, or SCN^- are present, the cluster grows to $[Au_{11}L_8X_2]^+$ or $Au_{11}L_7X_3$.

In the attempt to isolate an intermediate in the formation of gold cluster compounds, no anions were added during the reaction of gaseous gold atoms with L in a toluene solution. The hydroxide anion that is supposed to be present in $[Au_7L_7](OH)$ probably originates from traces of water in the toluene solution (only 10 ppm of H_2O in 300 mL of toluene are required) or of the inleak of air in the evaporating appa-

ratus. The 1+ charge of the Au_7 cluster was confirmed not only by the conductivity measurements and Hückel MO calculation on the bare Au_7 skeleton but also by its chemical behavior as discussed below.

$[Au_7L_7]^+$ can be observed in a ^{31}P{^{1}H} NMR experiment by adding an excess of L to an acetone solution of $[Au_8L_6I]PF_6$. The degradation of the octanuclear cluster proceeds similar to the $[Au_9L_8]^{3+} \leftrightarrow [Au_8L_8]^{2+}$ interconversion reactions:[5]

$$[Au_8L_6I]^+ + L(\text{excess}) \rightarrow$$
$$[Au_7L_7]^+ + [AuL_n]^+ \quad (n = 2\text{--}4)$$
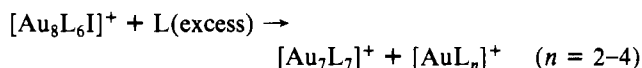
Since $[Au_8L_7]^{2+}$ and $[Au_8L_8]^{2+}$ do not degrade toward $[Au_7L_7]^+$ in the presence of phosphine, the substitution of a phosphine by an iodide in $[Au_8L_7]^{2+}$ is a requirement. Since $[Au_8L_6I]^+$ is thought to be isostructural with $[Au_8L_7]^{2+}$, analogously the addition of one phosphine to $[Au_8L_6I]^+$ is to be expected. The subsequent elimination of AuI results in the formation of $[Au_7L_7]^+$.

From ^{31}P{^{1}H} NMR experiments it has been shown that $[Au_7L_7]^+$ reacts quantitatively with 1 equiv of $AuLNO_3$ toward $[Au_8L_8]^{2+}$ and with 2 extra equiv of $AuLNO_3$ toward $[Au_9L_8]^{3+}$ via $[Au_8L_7]^{2+}$. In Scheme I, all reactions discussed in this paper are represented, showing interconversion reactions in the $Au_7 \leftrightarrow Au_8 \leftrightarrow Au_9$ series.

When $[Au_7L_7]^+$ is dissolved in ethanol, a slow conversion reaction toward $[Au_9L_8]^{3+}$ can be observed, via $[Au_8L_8]^{2+}$ and $[Au_8L_7]^{2+}$. This reaction probably proceeds through slow oxidation of the starting material into $[AuL]^+$, which will react subsequently according to Scheme I. Similar reactions occur in methylene chloride. $[Au_7L_7]^+$ is stable for hours in acetone or THF but reacts fast with AuLX (X = Cl, I, SCN) toward $[Au_{11}L_8X_2]^+$ and $Au_{11}L_7X_3$, as was shown by ^{31}P{^{1}H} NMR experiments. For $Au_{11}L_7I_3$, an X-ray structure analysis confirmed its identity.[25]

Conclusion

It has been suggested that the formation and reactions of gold clusters proceed via small intermediates containing 2–4 metal atoms. Attempts to isolate such a small intermediate were not successful but led to the discovery of two novel gold cluster compounds, the $[Au_8L_6I]^+$ and the $[Au_7L_7]^+$ cluster. Both compounds have been shown to be intermediates in the formation and/or reactions of gold cluster compounds.

Scheme I

(17) Albano, V. G.; Ceriotti, A.; Chini, P.; Ciani, G.; Martinengo, S.; Anker, W. M. *J. Chem. Soc., Chem. Commun.* **1975**, 859.

(18) Calabrese, J. C.; Dahl, L. F.; Chini, P.; Longoni, G.; Martinengo, S. *J. Am. Chem. Soc.* **1974**, *96*, 2614.

(19) Washecheck, D. M.; Wucherer, E. J.; Dahl, L. F.; Ceriotti, A.; Longoni, G.; Manassero, M.; Sansoni, M.; Chini, P. *J. Am. Chem. Soc.* **1979**, *101*, 6110.

(20) Alpress, J. G.; Saunders, J. V. *Surf. Sci.* **1967**, *7*, 1.

(21) Briant, C. L. *Faraday Discuss. Chem. Soc.* **1976**, *61*, 25.

(22) Vollenbroek, F. A.; van der Velden, J. W. A.; Bour, J. J.; Trooster, J. M. *Recl. Trav. Chim. Pays-Bas* **1981**, *100*, 375.

(23) van der Velden, J. W. A.; Bour, J. J.; Bosman, W. P.; Noordik, J. H. *J. Chem. Soc., Chem. Commun.* **1981**, 1218.

(24) Vollenbroek, F. A.; Bour, J. J.; Trooster, J. M.; van der Velden, J. W. A. *J. Chem. Soc., Chem. Commun.* **1978**, 907.

(25) Smits, J. M. M.; Beurskens, P. T.; van der Velden, J. W. A.; Bour, J. J., submitted for publication in *J. Crystallogr. Spectrosc. Res.*

(26) Beurskens, P. T.; Bosman, W. P. *J. Crystallogr. Spectrosc. Res.*, in press.

recording of the ^{197}Au Mössbauer spectra. The investigations were partly supported by the Netherlands Foundation for Chemical Research (SON), with financial aid from the Netherlands Organization for the Advancement of Pure Research (ZWO).

37336-35-9.

Contribution from the Department of Chemistry, Gorlaeus Laboratories, State University Leiden, Leiden, The Netherlands

Synthesis, Structure, and Magnetic Properties of Fluoride-Bridged Copper(II) Dimers. Crystal and Molecular Structures of Bis(μ-fluoro)bis[tris(3,4,5-trimethylpyrazole-N^2)copper(II)] Bis(tetrafluoroborate) and Bis(μ-fluoro)bis[(5-methylpyrazole-N^2)bis(3,5-dimethylpyrazole-N^2)copper(II)] Bis(tetrafluoroborate)

FREDERIK J. RIETMEIJER, RUDOLF A. G. DE GRAAFF, and JAN REEDIJK*

The molecular structures of the compounds [Cu$_2$F$_2$(tmpz)$_6$](BF$_4$)$_2$ and [Cu$_2$F$_2$(dmpz)$_4$(mpz)$_2$](BF$_4$)$_2$ (abbreviated as I and II, respectively, with tmpz = 3,4,5-trimethylpyrazole, dmpz = 3,5-dimethylpyrazole, and mpz = 5(3)-methylpyrazole), as determined by single-crystal X-ray analyses, are described. I was prepared from copper(II) tetrafluoroborate and tmpz. II was synthesized via partial substitution of dmpz ligands in [Cu$_2$F$_2$(dmpz)$_6$](BF$_4$)$_2$. I crystallizes in the monoclinic space group $P2_1/n$ with two formula units in a cell of dimensions $a = 11.514$ (4) Å, $b = 16.439$ (3) Å, $c = 13.159$ (3) Å, and $\beta = 101.82$ (2)°. II crystallizes in the monoclinic space group $P2_1/c$ with $a = 9.954$ (1) Å, $b = 11.862$ (2) Å, $c = 17.679$ (4) Å, $\beta = 99.45$ (1)°, and $Z = 2$. Reflection data were collected with an Enraf-Nonius CAD-4 single-crystal diffractometer and graphite-monochromatized Mo Kα radiation. Both structures were solved with use of conventional Patterson, Fourier, and least-squares refinement techniques. The final R factors were $R = 0.033$ and $R_w = 0.04$ for I (based on 2553 independent reflections) and $R = 0.035$ and $R_w = 0.047$ for II (based on 2258 independent reflections). The compounds are dimeric, with asymmetric difluoro bridges between the copper ions (in I, the two Cu-F distances are 1.911 (2) and 2.183 (2) Å; in II, they are 1.901 (2) and 2.195 (2) Å, respectively). In I, the Cu-F-Cu angle (94.59 (7)°) is slightly larger than in II (93.73 (8)°), as is the case for the Cu-Cu distances (in I, Cu-Cu = 3.0141 (8) Å; in II, Cu-Cu = 2.9962 (9) Å). In both compounds the coordination geometry is approximately square-based pyramidal. The fluoride ion with the largest distance to copper forms the apical ligand. The structures are compared with closely related structures of copper(II) dimers. The observed ligand field spectra are in agreement with square-pyramidal coordination geometry. Magnetic susceptibility measurements down to 2 K are indicative of a very small exchange interaction ($|J| < 0.5$ cm^{-1}). The EPR spectra are typical of Cu(II) dimers, showing both $\Delta m_s = 1$ and $\Delta m_s = 2$ transitions at various temperatures.

Introduction

In the last decade the increasing interest in magnetic exchange between paramagnetic transition-metal ions has simulated the study of dimeric, cluster, and linear-chain compounds. A detailed investigation of the magnetic interaction is easier in well-defined structures containing isolated magnetic units. Also favorable is the presence of simple bridging ligands such as OH$^-$, F$^-$, Cl$^-$, Br$^-$, oxamido(2–), oxamato(2–), acetato(1–), etc. The fluoride-bridged compounds are less well-known because of their inaccessibility. Since the introduction of BF$_4^-$ salt decomposition for the synthesis of fluoride-bridged transition-metal compounds, however, explorative work has resulted in a number of new compounds.[1-7] In this respect, the ligand-exchange method developed by Ten Hoedt, which involves the exchange of non-bridging ligands with other ligands, is of special interest.[6] We now report the crystal an molecular structures of the copper(II) dimers

Table I. Crystal Data for I

Cu$_2$C$_{36}$H$_{60}$N$_{12}$B$_2$F$_{10}$	$V = 2438$ Å^3
mol wt 999.6	$Z = 2$
monoclinic, space group $P2_1/n$	$d_{calcd} = 1.361$ g cm^{-3}
$a = 11.514$ (4) Å	$d_{obsd}{}^a = 1.34$ (2) g cm^{-3}
$b = 16.439$ (3) Å	μ(Mo Kα) = 10.1 cm^{-1}
$c = 13.159$ (3) Å	cryst dimens
$\beta = 101.82$ (2)°	$0.40 \times 0.35 \times 0.20$ mm

^{a} By the flotation method (CHCl$_3$/C$_2$H$_5$OH).

Table II. Crystal Data for II

Cu$_2$C$_{28}$H$_{44}$N$_{12}$B$_2$F$_{10}$	$V = 2059$ Å^3
mol wt 887.6	$Z = 2$
monoclinic, space group $P2_1/c$	$d_{calcd} = 1.431$ g cm^{-3}
$a = 9.954$ (1) Å	$d_{obsd}{}^a = 1.43$ (2) g cm^{-3}
$b = 11.862$ (2) Å	μ(Mo Kα) = 11.1 cm^{-1}
$c = 17.679$ (4) Å	cryst dimens
$\beta = 99.45$ (1)°	$0.25 \times 0.25 \times 0.50$ mm

^{a} By the flotation method (CHCl$_3$/C$_2$H$_5$OH).

[Cu$_2$F$_2$(tmpz)$_6$](BF$_4$)$_2$ (I) and [Cu$_2$F$_2$(dmpz)$_4$(mpz)$_2$](BF$_4$)$_2$ (II) together with spectroscopic and magnetic data. The results are compared with those of previous studies on related compounds.

Experimental Section

Syntheses. Commercial Cu(BF$_4$)$_2$·6H$_2$O and 3(5)-methylpyrazole (mpz, Aldrich) were used without further purification. 3,4,5-Trimethylpyrazole (tmpz) was prepared by a method described by

(1) Guichelaar, M. A.; Van Hest, J. A. M.; Reedijk, J. *Inorg. Nucl. Chem. Lett.* **1974**, *10*, 999-1004.
(2) Reedijk, J.; Jansen, J. C.; Van Koningsveld, H.; Van Kralingen, C. G. *Inorg. Chem.* **1978**, *17*, 1990-1994.
(3) Verbiest, J.; Van Ooijen, J. A. C.; Reedijk, J. *J. Inorg. Nucl. Chem.* **1980**, *42*, 971-975.
(4) Ten Hoedt, R. W. M.; Reedijk, J. *Inorg. Chim. Acta* **1981**, *51*, 23-27.
(5) Ten Hoedt, R. W. M.; Reedijk, J.; Verschoor, G. C. *Recl. Trav. Chim. Pays-Bas* **1981**, *100*, 400-405.
(6) Reedijk, J.; Ten Hoedt, R. W. M. *Recl. Trav. Chim. Pays-Bas* **1982**, *101*, 49-57.
(7) Reedijk, J. *Comments Inorg. Chem.* **1982**, *1* (6), 379-389.